REVEALING BONE DAMAGE USING RADIOGRAPHIC IMAGE REGISTRATION

[1]*Joost Kauffman,* [1]*Kees Slump,* [2]*Hein Bernelot Moens*

[1]j.a.kauffman@el.utwente.nl
[1]University of Twente, Dept. of Electrical Engineering, Drienerlolaan 5, Enschede, The Netherlands
[2]Ziekenhuisgroep Twente, Hengelo, The Netherlands

ABSTRACT

Bone damage assessment is frequently applied to monitor the activity of bone degenerative diseases such as rheumatoid arthritis and osteoarthritis. For an effective treatment it is important that small changes over time can be measured. Radiographs of hands and feet are often used for such measurements. Several scoring methods exist to measure bone and joint damage [1], but they are subjected to inter-observer and intra-observer variability. We present a method for comparing radiographs that have been taken at different moments in time. Using the segmentation algorithm presented in earlier work [2] we select corresponding regions of interest surrounding the bone to be analyzed. Both image selections taken at different time-points are aligned to each other with a registration algorithm [3]. After aligning the images, we visualize the difference by image subtraction. Since there is generally no information available about the setup of the radiographic system during both acquisitions, we compensate for differences in lighting. We do this by estimating an intensity transformation function based on the joint density function of both images. Experimental results with several follow-up radiographs show that we are able to visualize small erosions and changes in bone mineral density. To further improve the estimation of the intensity transformation function, we plan to use a calibration object in future research.

1. INTRODUCTION

Bone degenerative diseases such as rheumatoid arthritis and osteoarthritis cause pain, swelling, stiffness, and loss of function in the joints. Since bone damage is often irreversible, it is important to closely monitor the effects of treatments and to measure disease activity. Radiographs of hands and feet are generally used for this purpose, since they are often affected in an early stage. Several scoring methods have been proposed [1] to quantify joint damage in such radiographs. Some make use of classification scores for joint erosions and deformations, for example the Larsen score [4], and the Sharp/van der Heijde method [5]. Other methods are based on relative or absolute measurements, for example determining the carpal/metacarpal ratio [6], joint space width measurement and erosion volume estimation. In general these methods are time-consuming and depend on subjective visual readings [7]. An important property of a scoring method is its sensitivity for small changes. This sensitivity is partially inherent to the applied method, but generally also dependent on the experience and attentiveness of the human reader.

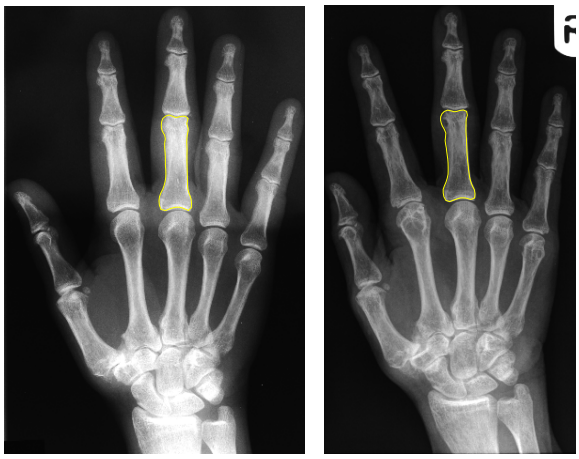

Figure 1: *Two radiographs of the same patient; the left is the baseline image, the right has been made several years later.*

With existing methods disease activity is determined indirectly by looking at changes in scores, rather than detecting radiographic differences directly. However, when two follow-up radiographs are displayed side by side, it is easy to overlook small erosions or differences in bone density. A comparative analysis becomes even more difficult when images have been acquired through different devices or with other settings. Even a change in the contrast and brightness settings may affect a reader's opinion. As nowadays more and more hospitals are working with digitized radiographs, new possibilities for radiographic analysis have become available. The analysis of radiographs on a computer screen has several advantages; e.g. regions of interest can easily be magnified, the contrast and brightness settings can be changed and special filters can be applied to enhance certain image features.

In this study we use image subtraction to reveal changes in

bone structures between follow-up hand radiographs. We achieve this by aligning a region of interest within both images and calculating the difference between the pixel intensities. In the field of image procession, this alignment procedure is referred to as 'image registration' [8]. The large variability in hand positioning makes it difficult to register two images entirely. Overlapping bone parts near the joints and differences in projection angle cause interfering artifacts when stringent elastic transformations are applied to one of the images. Therefore we restrict our analysis to rigid regions of interest, such as the individual bones. The images that we would like to compare have been taken at different time instances, typically with several years in between. It is not uncommon with such data that the radiographs have been acquired differently: the hospital's equipment may have been renewed or its settings changed, the patient might have gone to another hospital or the acquisition protocol may have been changed. This makes it difficult to compare radiographs directly, since illumination settings such as contrast and brightness may be different. We compensate for such differences by determining an intensity transformation function based on the joint histogram of the relevant images. Finally, the difference is determined through image subtraction and displayed to the operator by means of a color overlay in the radiograph that is examined.

2. METHOD

To illustrate our method we take two follow-up hand radiographs that have been made with several years in between. The third proximal phalanx is selected for this example, since it shows a clearly visible erosion at its distal end in the second radiograph. For the selection of the bone, we apply the algorithm that we have presented earlier to detect the rough bone outline in both images [2]. Figure 1 shows the detected outline of the selected bone. Next, we extract a rectangular region of interest (ROI) that fits the bones with 3 mm of extra space around the outlines. A rigid transformation is used to warp these ROIs to two new images A and B, as shown in Figure 2.
Both images are now roughly aligned. Due to small deviations in the detected contours, a small error may still be present. To further improve alignment, we apply an image registration method.

2.1. Image registration

A medical image registration algorithm is used to register the first image to the second, which is described in [3]. Although bones are mostly rigid, we allow subtle elastic transformations in the registration algorithm. This is necessary to correct for small, but smooth, contour variations caused by differences between the projection angles during acquisitions. By smoothing the deformation field we prevent the registration algorithm from applying strong local deformations that might conceal erosions.

Figure 3 shows the effect of the calculated deformation field on a mesh. The result of the registration is displayed in the checkerboard image of Figure 4.

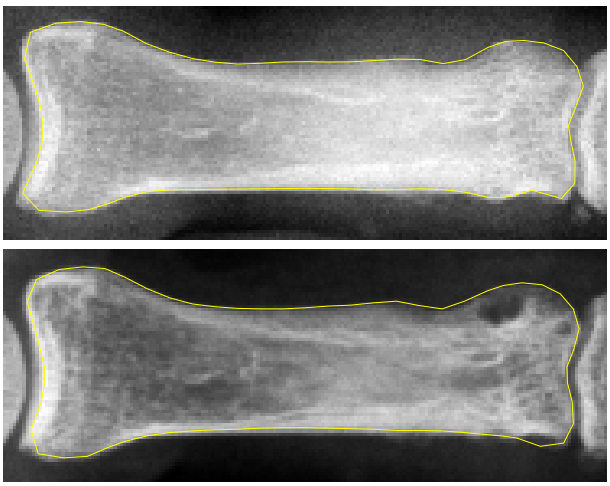

Figure 2: *The upper image shows reference image A, the baseline image, and the lower shows B made several years later.*

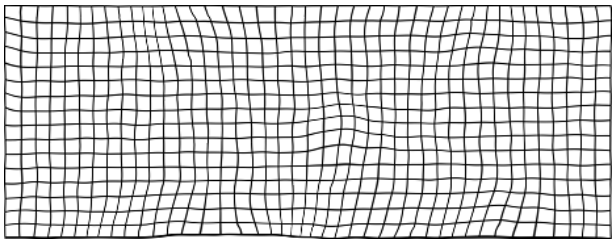

Figure 3: *The deformation field applied to a mesh.*

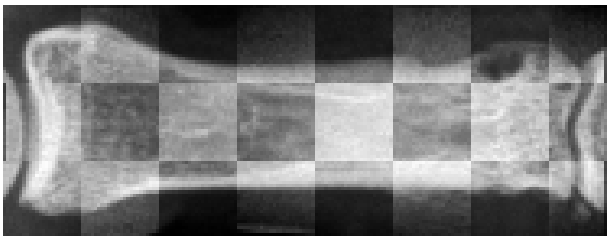

Figure 4: *Checkerboard view of registered source and target images.*

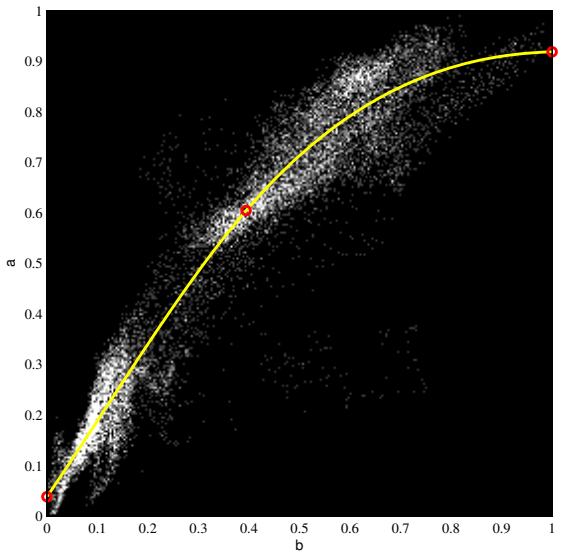

Figure 5: *The joint distribution in gray intensities and the fitted cubic spline $S(t)$ displayed by the yellow line. The red circles are the locations of the knots that define the spline.*

2.2. Intensity transformation function

After the images are registered, we want to compare the image intensities through subtraction. Since we lack information on how the images have been acquired, the relation between their intensity values is unknown. If there is only a difference in contrast and brightness, this relation would be linear. However, it is more likely that it is more complex, as the characteristics of radiographic imaging techniques are usually exponential.

The goal is to find an intensity transformation function that changes the pixel values of image B such that we can compare it to the intensities of *reference image* A. Since both images have been aligned, we can make use of the joint distribution $f_{A,B}(a, b)$, where a and b are values of corresponding pixels in image A and B. Figure 5 shows the joint distribution of the example images in a grey-scale image. For this purpose the image intensities have been made discrete by dividing them into 256 bins of equal size. The higher the displayed intensity, the higher the occurrence.

We estimate the intensity transfer function by fitting a cubic spline function $S(t)$ [9] to the data of the joint distribution. The spline that is fitted is defined by a knot vector $\mathbf{t}$ of three points with the following conditions:

$$t_1 = 0 \tag{1}$$

$$0 < t_2 < 1 \tag{2}$$

$$t_3 = 1 \tag{3}$$

$$S(t_1) < S(t_2) < S(t_3) \tag{4}$$

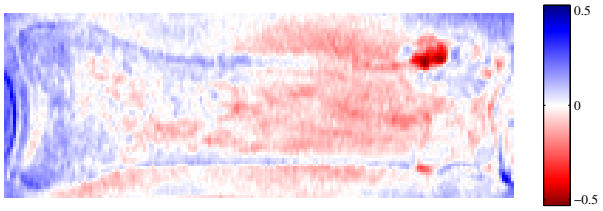

Figure 6: *Difference image normalized by the average intensity of the bone in image A.*

The begin and end conditions $S'(t_1)$ and $S'(t_3)$ are constrained to positive values, such that the curve is increasing. The spline is fitted to the joint distribution in a least squares manner using a reflective Newton method [10]. The fitted spline of the example is also displayed in Figure 5.

Next, we apply the intensity transformation to image B and calculate difference image D by subtracting image A:

$$D = S(B) - A \tag{5}$$

Since we do not have any information to be able to quantify the image intensities, we normalize the intensities by dividing them by the average intensity of the bone in image A. We note that this average may be inaccurate, since the intensity scale is likely to be slightly nonlinear. The resulting difference image is shown in Figure 6. A color mapping is used such that a decrease in bone density is colored red and an increase blue.

In this example the erosion is clearly visible, but in other cases this representation may still be difficult to interpret: the reader is easily distracted by small deviations caused by noise and differences in illumination. To enhance the readability of the results we add an alpha channel (transparency map) to the the colored difference image and use image B as background. The alpha channel image α_D is constructed from the difference image D by taking the absolute value and mapping the values between a lower and upper threshold (τ_1 and τ_2) to values between 0 and 1:

$$\alpha_D = \begin{cases} 0 & \text{if } |D| \leq \tau_1 \\ \frac{1}{\tau_2 - \tau_1}(|D| - \tau_1) & \text{if } \tau_1 < |D| < \tau_2 \\ 1 & \text{if } |D| \geq \tau_2 \end{cases} \tag{6}$$

Figure 7 displays the alpha channel for described example. This alpha channel is used to mix A and D by means of the following equation:

$$M = A(1 - \alpha_D) + \alpha_D D \tag{7}$$

The resulting mixed image M of our example is displayed in Figure 8.

As can be seen in the result, there are some strong differences visible at the adjacent bones. Optionally, we can

Figure 7: *Alpha channel* α_D.

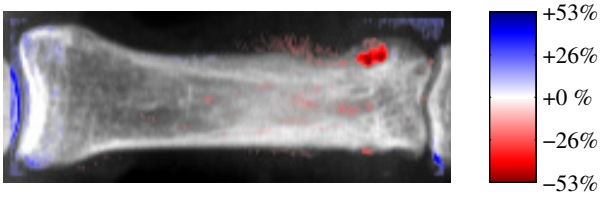

Figure 8: *Mixed image: image A and D with applied alpha channel. The difference is displayed as the percentage of the average intensity of the bone at baseline. Applied thresholds for alpha channel:* $\tau_1 = 0.1$ *and* $\tau_2 = 0.3$.

remove these regions by applying a mask using the initially detected contours. But this also means that possible changes near the edges of bone become invisible. One may also note the thin blue edge at the metacarpal head. It is likely that this is the result of joint space narrowing, which indicates the loss of cartilage in the joint.

3. RESULTS

Experiments with several follow-up radiographs show that erosions and changes in bone mineral density can be visualized. Figure 9 shows four follow-up radiographs of a third metacarpal bone. The top image is the baseline image and is used as the reference image. The following three images have been made after 1, 2 and 5 years. The pixel size is 0.25 mm for all images.
The described method was applied as follows. Firstly, we registered the baseline image the other three images. Secondly, we corrected the intensities of the latter three images to match the baseline image; see Figure 10. Finally, for each image we calculated the difference with the baseline image. Figure 11 shows the differences as overlays. The alpha channel thresholds are: $\tau_1 = 0.1$ and $\tau_2 = 0.4$.

4. DISCUSSION

Our experiments show that image subtraction techniques can be used to visualize local changes in bone density. Such changes are important indicators of disease activity

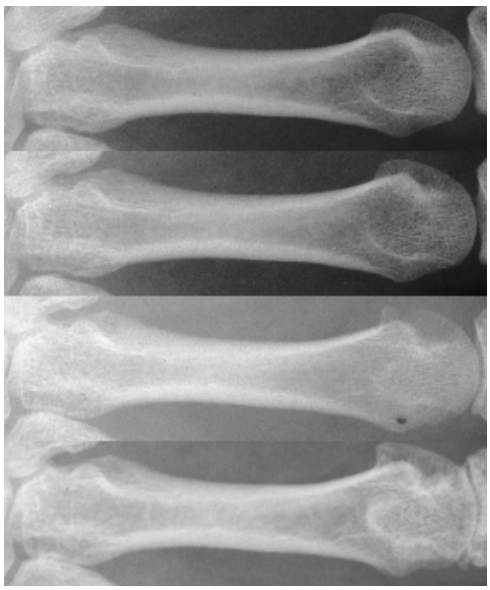

Figure 9: *Original series of follow-up images of a third metacarpal bone. The baseline image is at the top, followed by images made after 1 year, 2 years and 5 years.*

Figure 10: *The same images as in Figure 9, but with applied intensity transformation to match the intensities of the baseline image.*

and may show the effects of treatments. The presented method of displaying intensity differences by means of a colored overlay may offer a useful aid to the reader during radiographic analysis.
Within the current method the joint distribution is used to estimate the intensity transformation function for match-

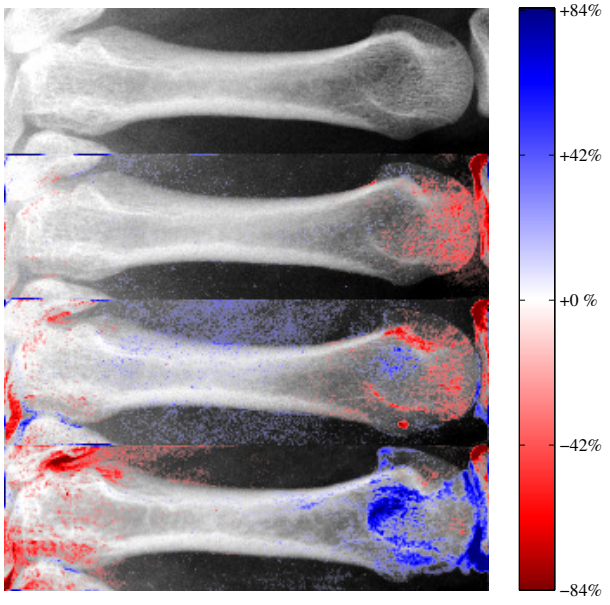

Figure 11: *Images as in Figure 10 with difference overlay. The difference is in percentage of the average intensity of the bone at baseline.*

ing the illumination settings between both images. With this method it is difficult to detect uniform changes in bone density. Also, large changes between consecutive images may result in a poor estimation of the intensity transformation function. Ideally a calibration object should be placed in the image area during image acquisition. Matching the illumination properties of the calibration object instead of the bones may solve this problem. In future research we plan to use an aluminum wedge for this purpose.

Currently, intensity differences have been quantified with a relative measure: as a percentage of the average bone intensity at baseline. For absolute measurements there should be an accurate bone density measurement for at least one of the time instances. For example, this could be done with a DEXA scan.

5. REFERENCES

[1] J.T. Sharp, "An overview of radiographic analysis of joint damage in rheumatoid arthritis and its use in meta-analysis," *The Journal of Rheumatology*, vol. 27, no. 1, pp. 254–260, 2000.

[2] J.A. Kauffman, C.H. Slump, and H.J. Bernelot Moens, "Segmentation of hand radiographs by using multi-level connected active appearance models," in *Medical Imaging 2005: Image Processing*, J. Michael Fitzpatrick and Joseph M. Reinhardt, Eds., San Diego, CA, USA, 2005, vol. 5747, pp. 1571–1581, SPIE.

[3] S. Periaswamy and H. Farid, "Elastic registration in the presence of intensity variations," *IEEE Transactions on Medical Imaging*, vol. 22, no. 7, pp. 865–874, 2003.

[4] A. Larsen, "How to apply Larsen score in evaluating radiographs of rheumatoid arthritis in long-term studies," *The Journal of Rheumatology*, vol. 22, no. 10, pp. 1974–1975, 1995.

[5] D. van der Heijde, "How to read radiographs according to the Sharp/van der Heijde method," *The Journal of Rheumatology*, vol. 27, no. 1, pp. 261–263, 2000.

[6] D.E. Trentham and A.T. Masi, "Carpo:metacarpal ratio. A new quantitative measure of radiologic progression of wrist involvement in rheumatioid arthritis," *Arthritis and Rheumatism*, vol. 19, no. 5, pp. 939–944, 1976.

[7] D.L. Scott, "Radiographs in Rheumatoid Arthritis," *International Journal of Advances in Rheumatology*, vol. 1, no. 1, 2003.

[8] B. Zitova and J. Flusser, "Image registration methods: a survey," *Image and Vision Computing*, vol. 21, no. 11, pp. 977–1000, 2003.

[9] J.H. Ahlberg, E.N. Nilson, and J.L. Walsh, *The theory of spline functions and their applications*, Mathematics in Science and Engineering, New York: Academic Press, 1967, 1967.

[10] T.F. Coleman and Y. Li, "A Reflective Newton Method for Minimizing a Quadratic Function Subject to Bounds on Some of the Variables," *SIAM Journal on Optimization*, vol. 6, no. 4, pp. 1040–1058, 1996.